

## Modelling and Control of a Grid Connected Photovoltaic System

N. Hamrouni and A. Cherif

Laboratory of Electrical Systems 0S2E, High Engineering Academy of Tunis PB 37,  
 1002 Le Belvedere-Tunis, Tunisia

**Abstract:** This study presents a simulation model of the electric part of a grid connected photovoltaic generator. The model contains a detailed representation of the main components of the system that are the solar array, boost converter and the grid side inverter. A proper control of the DC/DC converter is developed in order to extract the maximum amount of from the photovoltaic generator. The grid interface inverter transfers the energy drawn from the PV module into the grid by keeping common dc voltage constant. The PQ control approach has been presented for the inverter. Modelling and control is carried out using the causal informational graph method. The simulation results under MATLAB/SIMULINK show the control performance and dynamic behaviour of grid connected photovoltaic system.

**Key words:** PV, inverter, grid, MPPT, CIG, PQ

### INTRODUCTION

Photovoltaic power supplied to the utility grid is gaining more and more visibility, while the world's power demand is increasing. It registers an exponential increase with Germany and Japan leading the list of the countries having the largest capacity installed. Unconditional availability of the power source the environmental friendliness of these systems are their major advantages over the traditional energy sources such as oil and natural gas, but their efficiency and controllability stand as the major drawbacks. In addition to this, the transmission system operators are imposing tough standards (IEC 1727, 2002) when system PV is connected the utility network. Many demands such as power system stability and power quality are primary requests. As a consequence, large research efforts are put into the control of these systems in order to improve their behaviour. All photovoltaic systems are interfacing the utility grid through a voltage source inverter (Blaabjerg *et al.*, 2004) and a boost converter. Many control strategies and controller types (Liang *et al.*, 2002; Mattavelli and Marfao, 2004; Kanellos and Hatziaargyriou, 2002) have been investigated. Authors have been demonstrated that in the case of grid frequency or voltage fluctuations, there are problems in controller of the grid current and power factor.

One of the most common control strategies structures applied to decentralized power generator is based on voltage oriented control employing a controller for the dc link voltage and a controller to regulate the injected current to the utility network (Kazmierkowrki *et al.*, 2002).

The system components and power control scheme were modelled in terms of dynamic behaviours. The modelling and control methods of the grid connected photovoltaic system chosen in our subject, rest on the Causal Informational Graph and its wide form the Macroscopic Energy Representation. The proposed models were implemented in Matlab/simulink. This study describes the dynamic performance of the PV generator connected through inverters to distribution network under standard climatic conditions ( $1000\text{W m}^{-2}$  and  $25^{\circ}\text{C}$ ).

By the means of graphic symbolisms methods evoked in we will develop the elementary as well as the global models of the grid connection photovoltaic system. Consequently, by the inversion of the found model, we will calculate the control laws allowing the maximum extraction of photovoltaic power and the connection to the electrical supply network.

Converters interfacing PV module with the grid involves tow major tasks. One is to ensure that the PV module is operated at the maximum power point. The other is to inject a sinusoidal current to the grid. These tasks are further reviewed in this study. Simulating results are obtained for the normal regime.

### SYSTEM CONFIGURATION

Figure 1 shows the power converter structure used to interface the photovoltaic array with the power grid. The first stage is the boost converter, which will raise the relatively low solar voltage to a level suitable (550V) for

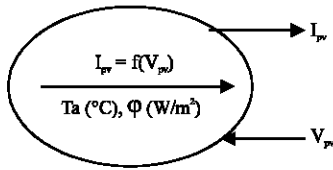


Fig.1 : MER of PVG

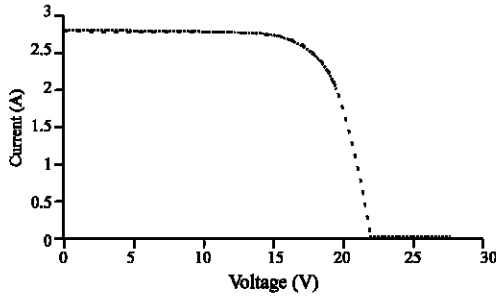


Fig. 2: I-V curve of photovoltaic generator PVG

the dc link directly connected to the inverter. The second stage is the DC to AC converter that operates in a current controlled mode which will inject unity power factor current to the grid. The inverter should be able to supply a continuous power from the dc link bus to a three-phase utility line (220V/50Hz). An output L filter is employed to reduce the ripple components due to PWM switching operation.

**PV generator:** Using the Causal Informational Graph (CIG), the mathematical model of Photovoltaic Generator (PVG) (Harmouni *et al.*, 2004) is presented on the Fig. 2. The model inputs are the solar irradiation [ $W m^{-2}$ ], the ambient temperature [ $^{\circ}C$ ], the photovoltaic generator voltage [V] and the wind speed [ $m s^{-1}$ ], whereas the only output is the photovoltaic current which supplied by the panel [A].

For standard climatic conditions, the simulated I-V characteristic for a photovoltaic generator formed by crystal mono silicon cells (40 series cells), is presented by the Fig. 2. Boost Converter

**Boost converter:** The MER of the DC/DC converter and command system are given by Fig. 2. The DC/DC reveals two power accumulation elements and thus two variables to control. They are the photovoltaic voltage  $V_{pv}$  and the inductor current  $I_l$ .

According to the Fig. 3, a mathematical model describing the boost converter connected photovoltaic generator may be written in the following from:

$$\begin{pmatrix} V_m \\ i_{dc} \end{pmatrix} = m \begin{pmatrix} V_{dc} \\ i_l \end{pmatrix} \quad (1)$$

$$\frac{dV_{pv}}{dt} = \frac{1}{C_{pv}}(i_l - i_{pv}) \quad (2)$$

$$\frac{di_l}{dt} = \frac{1}{L_{pv}}(V_m - V_{pv}) - \frac{R_{pv}}{L_{pv}}i_l \quad (3)$$

**DC link:** Generally, the DC link voltage oscillates between two levels depending on the operating climatic conditions, i.e., ambient temperature and irradiance. It is governed by the following equation:

$$\frac{dV_{dc}}{dt} = \frac{1}{C_{dc}}(i_{dc} - i_{ond}) \quad (4)$$

Where:

- $C_{dc}$  = Capacitance of the capacitor [F],
- $I_{dc}$  = Output current of MPPT regulator [A],
- $I_{ond}$  = Input current of DC/AC inverter [A],

**Inverter:** The grid side inverter has six IGBTs as switching devices. It has an L harmonic filter at its terminal to reduce the current distortion. The inverter must act as a power controller between the dc link and the utility (Koutroulis *et al.*, 2001; Nergard *et al.*, 2002).

The basic inverter models formulated in the literature, for these devices functioning, are the discrete and average models (Zhou and Wang, 2002). In spite of its disadvantages, the average model remains often used since it gives satisfaction for the analysis and the design of the control devices.

DC/AC is a double modulator (Francois, 2003) of variable states: Voltage  $U_{m1}$  and  $U_{m2}$  are modulations of dc link voltage and the input inverter current is a modulation of the network currents  $i_{r1}$  and  $i_{r2}$ . They can be described by Eq. 5 and 6.

$$[I_{ond}] = [m1 \ m2] \begin{bmatrix} i_{r1} \\ i_{r2} \end{bmatrix} \quad (5)$$

$$\begin{pmatrix} U_{m1} \\ U_{m2} \end{pmatrix} = \begin{pmatrix} m1 \\ m2 \end{pmatrix} V_{dc} \quad (6)$$

$m1$  and  $m2$  are obtained from the subtraction of two connection functions having a binary value (0,1). Their fields of definition are thus  $\{-1, 0, 1\}$ .

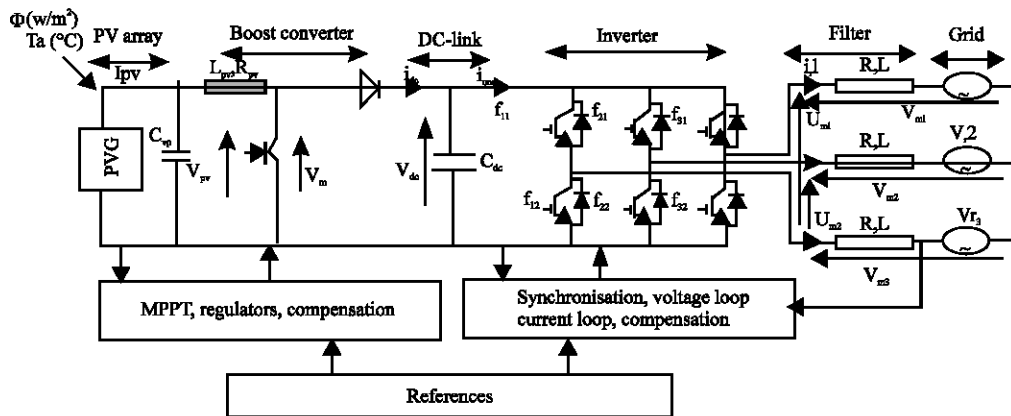


Fig. 3: General diagram of grid connected photovoltaic system

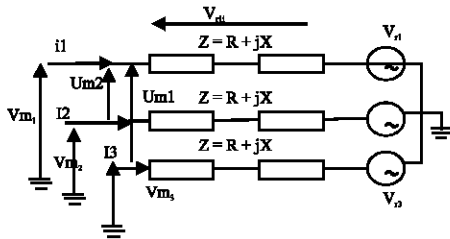


Fig. 4: Thévenin equivalent circuit of the utility grid

$$\begin{aligned} m1 &= f11 - f13 \\ m2 &= f12 f13 \end{aligned} \quad (7)$$

If the receiver is cabled out of star, the simple voltage will depend on the modulated voltages which are applied by the matrix of switches. They can be expressed as follow:

$$\begin{aligned} Um1 &= Vm1 - Vm3 \\ Um2 &= Vm2 - Vm3 \end{aligned} \quad (8)$$

If the receiver impedances have the same value, then the modulated simple voltage system can be described by the following equation:

$$\begin{pmatrix} Vm1 \\ Vm2 \end{pmatrix} = \frac{1}{3} \begin{pmatrix} 2 & -1 \\ -1 & 2 \end{pmatrix} \begin{pmatrix} Um1 \\ Um2 \end{pmatrix} \quad (9)$$

**Grid:** The unit formed by the energy transport line and all the connection transformers between the various voltage levels, will be indicated by network (Fig. 4). It is modelled by a Thévenin equivalent circuit composed by a sinusoidal voltage source (50Hz, 220V) in series with an impedance ( $Z = R + jX$ ). It includes all the impedances which are indicated above and the output inverter filter L. This circuit is fed by the inverter output voltage.

## CONTROL SYSTEM

**PV side power control:** According to the propriety of the CIG the command low is obtained by inversion of the model. It is composed by a control system of the energy stored in the inductor  $L_{pv}$  and the capacitance  $C_{pv}$ . In order to extract the maximum amount energy, the PV system must be capable of tracking the solar arrays Maximum Power Point (MPP) that varies with the solar radiation value and temperature. For the tuning of the power, it should be noticed that there is not explicit reference power, because photovoltaic power varies with the climatic conditions.

However, to extract the maximum photovoltaic current, the generator voltage must be adjusted according to the solar radiation. This adjustment is made possible while; varying the transistor cyclic ratio, carrying out a regulation of the generator voltage ( $V_{pv}$ ) and the inductor current ( $i_l$ ). MPPT requires the measurement of the photovoltaic voltage and current. The finality of MPPT law is to find the adequate voltage  $V_{pv}^*$ , which boost converter must impose to the system. The reference voltage will be determined by the calculation of two adequate controllers, 2 compensator blocs and an MPPT loop (Fig. 5).

The inversion of previously Eq. 2 and 3, representing the voltage and current variation respectively in the capacitor  $C_{pv}$  and the inductance  $L_{pv}$ , gives the optimal command of current and voltage. The voltage control loop with the photovoltaic current compensation gives the current reference  $i_l^*$ , whereas the current control loop with the photovoltaic voltage compensation gives the voltage reference  $V_{pv}^*$  as indicated in (10) and (11)

$$i_l^* = PI(V_{pv}^* - V_{pv}) + i_{pv} \quad (10)$$

$$V_{pv}^* = PI(i_l^* - i_l) + V_{pv} \quad (11)$$

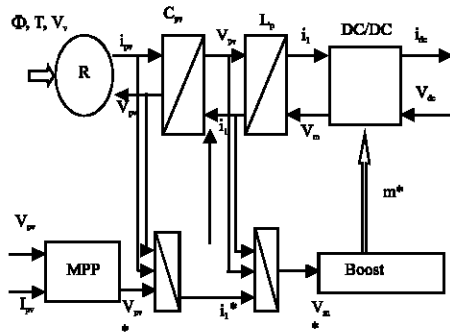


Fig. 5: PV side converter controller

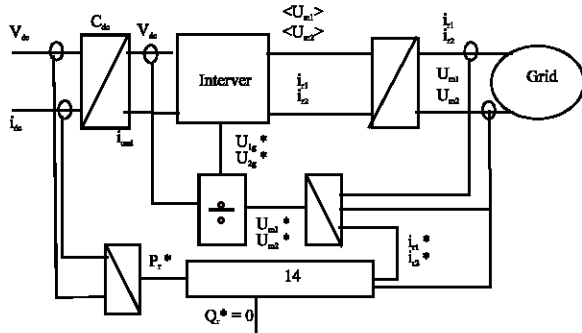


Fig. 6: Grid side converter controller

The controller parameters are chosen to maintain constant photovoltaic voltage and to minimize the current ripple. The boost converter command is obtained by the inversion of the equation No. 1. It may be written in the following form:

$$m^* = \frac{V_m^*}{V_{dc}} \quad (12)$$

**Grid side power control:** In grid connected control mode, basically all the available power that can be extracted from the PV generator is transferred to the grid. The control structure for grid connected control mode is shown in Fig. 6. Standard PI controllers are used to regulate the inverter output currents in the abc synchronous frame in the inner control loops and the dc voltage in the other loop.

The reference reactive power is typically used to zero in order to achieve zero phase angle between voltage and current and so unity power factor can be achieved. The dc link voltage control is acting to supply the reference active power. The output of the current controllers sets the voltage reference for an average conversion control method that controls the switches of the grid inverter. Synchronous with grid is achieved by using a Phase Locked Loop (PLL) as described (Yann, 2005). The principle of the PLL is described in Fig. 7.

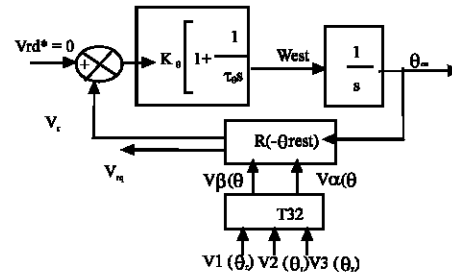


Fig. 7: Three phase PLL structure

**Voltage loop:** We exploit the causal informational graph properties as well as the developed equations in paragraph D to calculate the command laws. The direct inversion of the relation (4) gives the inverter input reference current  $i_{ond}$  (Yann, 2005). It can be described by the following equation:

$$i_{ond}^* = V_{dc} - PI(V_{dc}^* - V_{dc}) \quad (13)$$

To maintain constant the dc link voltage necessary to guarantee the excellent operation of the grid interface inverter without using a voltage transformer, we have recourse to use a proportional integral corrector. It is parameterized according to the capacitor value and the dynamics of the regulation loop. We can equalize the transfer function between the current  $i_{ond}$  and  $i_{ond}^*$  to a first order function. In general the current tuning dynamics is very high compared to that of the voltage, so it is possible to consider it as infinite for the synthesis of the corrector.

The reference active power injected to the electrical supply network is equal to:

$$P_r^* \approx i_{ond}^* \hat{V}_{dc} \quad (14)$$

Network reference currents, in Park frame, are given by the following relation (Hamrouni *et al.*, 2004):

$$\begin{bmatrix} i_{rd}^* \\ i_{rq}^* \end{bmatrix} = \frac{1}{V_{rq}^2 + V_{rd}^2} \begin{bmatrix} P_r^* & -Q_r^* \\ Q_r^* & P_r^* \end{bmatrix} \begin{bmatrix} V_{rd} \\ V_{eq} \end{bmatrix} \quad (15)$$

**Current loop:** In this study we will not detail the algorithm controls of the inverter such as the synthesis of the conversion modulators and the connection generators (Francois, 2003). The studied control device architecture is limited to the inversion of the average conversions equivalent model. The inverter is supposed commandable; the applied external controls to the switches are confused with the open or closed switches idealized states.

For a given dc link voltage  $V_{dc}$ , the instantaneous average value of composed voltage ( $U_{m1}$  and  $U_{m2}$ ) is directly dependent of the average value of the conversion functions  $m_{1g}$  and  $m_{2g}$ . By a direct inversion of the relation (6), we can determine the instantaneous average value of the conversion function references:

$$\begin{pmatrix} m_{1g}^* \\ m_{2g}^* \end{pmatrix} = \frac{1}{V_{dc}} \begin{pmatrix} U_{m1}^* \\ U_{m2}^* \end{pmatrix} \quad (15)$$

This linearization is static in the case when the dc link voltage is constant, and dynamic when is variable. For the studied case, the composed voltage  $U_{m1}$  and  $U_{m2}$  state are related to the dc link voltage regulator performances. The simple voltage control is carried out by a direct inversion of the relation (8) which gives:

$$\begin{pmatrix} U_{m1}^* \\ U_{m2}^* \end{pmatrix} = \begin{pmatrix} 2 & 1 \\ 1 & 2 \end{pmatrix} \begin{pmatrix} V_{m1}^* \\ V_{m2}^* \end{pmatrix} \quad (16)$$

The simple reference voltages  $V_{m1}^*$  and  $V_{m2}^*$  for each network phase can be expressed as follow:

$$\begin{pmatrix} V_{m1}^* \\ V_{m2}^* \end{pmatrix} = \begin{pmatrix} V_{r1}^* \\ V_{r2}^* \end{pmatrix} + \begin{pmatrix} v_{r1} \\ v_{r2} \end{pmatrix} \quad (17)$$

The filter and the line network impedance, formed by the equivalent resistance and inductance, is a power accumulation system. It connects the grid to the inverter. The simple voltage control of this impedance is obtained by the following equation:

$$\begin{pmatrix} v_{r1}^* \\ v_{r2}^* \end{pmatrix} = C_i(s) \begin{pmatrix} i_{r1}^* - i_{r1} \\ i_{r2}^* - i_{r2} \end{pmatrix} \quad (18)$$

The network current controller choice is made according to the regulation objectives and the network impedance. In order to synthesize the corrector  $C_i(s)$ , we supposed the following assumption (Francois, 2003):

$$\begin{pmatrix} V_{m1}^* \\ V_{m2}^* \end{pmatrix} \approx \begin{pmatrix} V_{m1} \\ V_{m2} \end{pmatrix} \quad (19)$$

By exploiting the preceding relations, we develop the control loop of current which circulates in each network phase. This control supposes the compensation of the network simple voltage  $V_{r1}$  and  $V_{r2}$ .

**Synchronisation:** The philosophy of the Park PLL is illustrated in Fig. 7. In this PLL, the phase angle is detected by synchronizing the PLL rotating reference

frame and the utility voltage vector. Setting the direct axis reference voltage  $v_{rd}^*$  to zero results in the lock in off the PLL output on the phase angle of the utility voltage vector. The output of the PI controller is the inverter output frequency that is integrated to obtain the inverter phase angle  $\theta_{est}$ . In addition, the instantaneous frequency and amplitude of the voltage vector are also determined. When the difference between grid phase angle  $\theta_r$  and the inverter phase angle  $\theta_{ond}$  is reduced to zero ( $\Delta\theta = 0$ ), the PLL became active (Francois, 2003) and we obtain:

$$V_{rd} = 0 \text{ and } V_{rq} = -\sqrt{3} V_r \quad (20)$$

In order to determine the PI controller, we refer to the equivalent linear model using  $\sin(\Delta\theta) \approx \Delta\theta$ .

## RESULTS AND DISCUSSION

A complete Simulink-Matlab simulation of the closed loop photovoltaic system including the global and command previously studied has been carried out with the following parameters:

Voltage grid 220V/50Hz,  
Filter and grid impedance:  $R = 2\Omega$ ,  $L = 0.002H$ ,  
Boost converter:  $R_{pv} = 1\Omega$ ,  $L_{pv} = 24.9e-4H$ ,  $C_{pv} = 5e-3F$  Dc link capacitance:  $C_{dc} = 910-3F$ ,

The PV generator is composed of 3 parallel and 20 series modules. Those modules are polycrystalline. Each module is formed by 40 series cells.

The results of simulation studies, obtained under standard climatic conditions ( $1000W m^{-2}$  and  $25^\circ C$ ), showed that satisfactory performance could be expressed from the demonstration system. The following figures show the results from some of the simulation results studies, selected to demonstrate the more significant aspects of system behaviour. Figure 8 shows the DC bus voltage regulated at 550V when the PVG is operating in grid connected mode. Figure 9 shows the transient and permanent response of the PVG. It also shows the maximal power supplied by the PVG in permanent functioning mode. Figure 10 and 11 show the injected active and reactive power. Those figures show a good performance of the current loop. As it might be noticed in Fig. 12, there isn't a phase leading/lagging between grid side line current and voltage. This makes the importance of the PLL loop for grid connected photovoltaic system.

The active power injected to the grid (2550W) is equal to maximal power provided by the PVG (2550W), because we are supposed that, in our modelling studies, there aren't losses in the system.

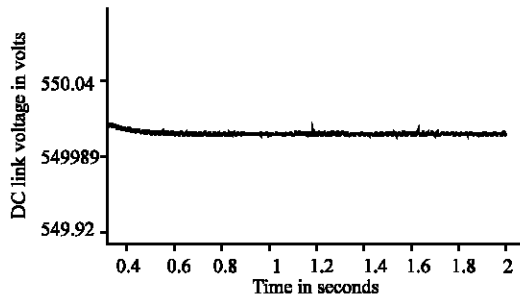


Fig. 8: DC link voltage

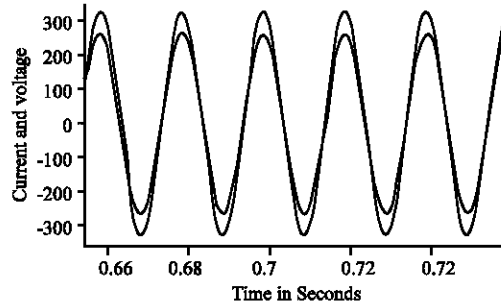


Fig. 12: Grid side line current (\*50) and voltage

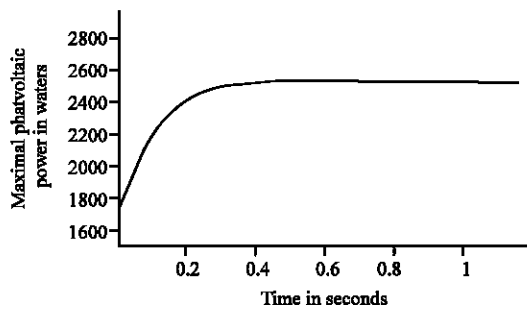


Fig. 9: Maximal photovoltaic power

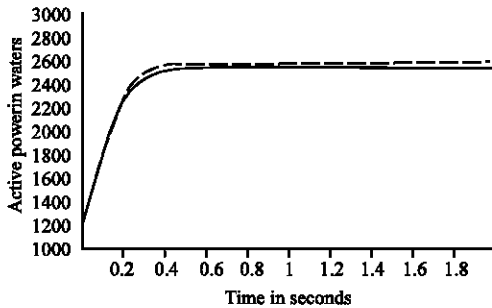


Fig. 10: Variation of the active power (reference/measure) injected in the grid

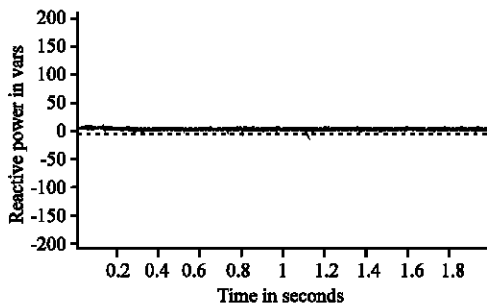


Fig. 11: Variation of the reactive power (reference/measure) injected in the grid

### CONCLUSION

This study treats an approach of modelling and control of a grid connected photovoltaic system. A causal informational graph method and its proprieties are permitted to determine all elementary models and to calculate the PV-side and grid-side controllers. In this way, an MPPT controller is used to extract the optimal photovoltaic power, a current and a dc link voltage regulator are used to transfer the photovoltaic power and to synchronise the output inverter with the grid. The simulated model and the results, obtained for standard operating conditions, are photovoltaic.

### REFERENCES

- Blaabjerg, F., Z. Chen and S. Kjaer, 2004. Power electronics as efficient interface in dispersed power generation systems, IEEE. Trans. Power Elec., 19: 1184-1194.
- Francois, B., 2003. Conception des dispositifs de commandes des convertisseurs de puissance par modulation directe des conversions. Perspectives pour l'insertion de production d'énergie dispersée dans les réseaux électriques, Habilitation à diriger des recherches, UST-Lille.
- Hamrouni, N., M. Jraidi, A. Cherif, A. Dhouib, 2004. Modelling, Simulation and Control of PV Pumping System, ELECTRIMACS, Hammemet-Tunisia.
- IEC 1727, 2002. Characteristics of the utility interface for Photovoltaic (PV) systems.
- Kanellos, F. and N. Hatziaegyriou, 2002. A New control Scheme for variable speed wind turbines neural networks, IEEE. Power Eng. Soc. Winter Meeting, 1: 360-365.
- Kazmierkowski, M., R. Krichnen and F. Belaabjerg, 2002. Control in power Electronics-Selected Problems. Academic Press.
- Koutroulis, E., J. Chatzakis, K. Kalaitzaks and N.C. Voulgaris, 2001. A bidirectionnel, Sinusoidal, high frequency inverter design, IEEE. Proceeding Electrical Power Applied, Vol. 148.

- Liang, J., T. Green, G. Weiss and Q.C. Zhong, 2002. Evaluations of repetitive control for power quality improvements of distributed generation, In: Proc. PESC, Cairns, Qld, 4: 1803-1808.
- Nergard, A. T., J.F. Ferrell, L.G. Leslie and Jih-Sheng Lai, 2002. Design considerations for 48V fuel cell to split single phase inverter system with ultra capacitor energy storage, in Conf. Rec. Power Electronics Specialists Conference, pesc 02. 2002 IEEE 33 Annu., 4: 2007-2012.
- Yann Pankow, 2005. Etude de l'intégration de la production décentralisée dans les réseaux Basse Tension. Application au générateur photovoltaïque, Thèse de Doctorat, ENSAM, Lille-France.
- Zhou, K. and D. Wang, 2002. Relationship between space vector modulation and three phase carrier-based pwm: A comprehensive analysis. IEEE. Trans. Indus. Elec., pp: 49.